

Levodopa-Induced Dyskinesia in Parkinson Disease Specifically Associates With Dopaminergic Depletion in Sensorimotor-Related Functional Subregions of the Striatum

Miguel A. Labrador-Espinosa, MSc, *† Michel J. Grothe, PhD, *† Daniel Macías-García, MD, *†
 Silvia Jesús, PhD, *† Astrid Adarmes-Gómez, MD, *† Laura Muñoz-Delgado, MD, †
 Paula Fernández-Rodríguez, MD, ‡ Juan Francisco Martín-Rodríguez, PhD, *†§ Ismael Huertas, PhD, *
 David García-Solís, MD, ‡ and Pablo Mir, PhD*†

Purpose: To determine whether the development of levodopa-induced dyskinesia (LID) in Parkinson disease (PD) specifically relates to dopaminergic depletion in sensorimotor-related subregions of the striatum.

Methods: Our primary study sample consisted of 185 locally recruited PD patients, of which 73 (40%) developed LID. Retrospective ¹²³I-FP-CIT SPECT data were used to quantify the specific dopamine transporter (DAT) binding ratio within distinct functionally defined striatal subregions related to limbic, executive, and sensorimotor systems. Regional DAT levels were contrasted between patients who developed LID (PD + LID) and those who did not (PD-LID) using analysis of covariance models controlled for demographic and clinical features. For validation of the findings and assessment of the evolution of LID-associated DAT changes from an early disease stage, we also studied serial ¹²³I-FP-CIT SPECT data from 343 de novo PD patients enrolled in the Parkinson Progression Marker's Initiative using mixed linear model analysis.

Results: Compared with PD-LID, DAT level reductions in PD + LID patients were most pronounced in the sensorimotor striatal subregion ($F = 5.99$, $P = 0.016$) and also significant in the executive-related subregion ($F = 5.30$, $P = 0.023$). In the Parkinson Progression Marker's Initiative cohort, DAT levels in PD + LID ($n = 161$, 47%) were only significantly

reduced compared with PD-LID in the sensorimotor striatal subregion ($t = -2.05$, $P = 0.041$), and this difference was already present at baseline and remained largely constant over time.

Conclusion: Measuring DAT depletion in functionally defined sensorimotor-related striatal regions of interest may provide a more sensitive tool to detect LID-associated dopaminergic changes at an early disease stage and could improve individual prognosis of this common clinical complication in PD.

Key Words: dopamine transporter (DAT), FP-CIT, levodopa-induced dyskinesia, Parkinson disease, SPECT

(*Clin Nucl Med* 2021;00: 00–00)

Levodopa-induced dyskinesia (LID) is one of the major motor complications related to dopaminergic treatment in patients with Parkinson disease (PD)^{1,2} and is associated with significant disability and reduced quality of life.³ Levodopa (L-DOPA)-induced dyskinesia affects approximately 40% of patients on chronic L-DOPA treatment^{4,5} and is characterized by involuntary, purposeless, and predominantly choreiform movements arising initially on the more affected body side.⁶ In terms of risk factors, high L-DOPA doses, duration of treatment, younger age at onset of PD, the severity of motor symptoms, and female sex, among other contributors, have been associated clinically with LID.^{7–9}

Although the pathophysiology of LID is still not clear, a widely discussed model hypothesizes that low intrastriatal dopamine caused by the degeneration of nigrostriatal dopaminergic projections, along with high plasma and extracellular concentrations of L-DOPA, is closely involved in the development of LID.^{6,10–12} The dissociation between these factors may provoke plastic changes in striatal dopaminergic neuron signaling that lead to abnormal firing patterns between the basal ganglia and the motor cortex, causing excessive disinhibition of thalamocortical neurons and overactivation of the motor cortex¹³ (Fig. 1).

In line with this model, neuroimaging studies could evidence a critical role of striatal dopaminergic denervation in the development of LID through molecular imaging of dopamine transporter (DAT) density using ¹⁸F-FP-CIT PET or ¹²³I-FP-CIT SPECT. Specifically, lower DAT levels in the putamen, but not in the caudate or ventral striatum, have been shown to predict the development of LID in de novo PD patients.¹⁴ Indeed, regional striatal DAT level depletion could also predict the timing of LID onset,¹⁵ and a higher asymmetry index of the posterior putamen region has been associated with slower changes in L-DOPA doses.¹⁶ However, considerable controversy still exists with respect to the exact striatal subregions that are most closely involved in the development of LID. For example, a recent longitudinal imaging study found that the dopaminergic depletion involved in LID development is not

Received for publication August 31, 2020; revision accepted January 28, 2021. From the *Unidad de Trastornos del Movimiento, Servicio de Neurología y Neurofisiología Clínica, Instituto de Biomedicina de Sevilla, Hospital Universitario Virgen del Rocío/CSIC/Universidad de Sevilla, Seville; †Centro de Investigación Biomédica en Red sobre Enfermedades Neurodegenerativas (CIBERNED), Madrid; ‡Unidad de Medicina Nuclear, Hospital Universitario Virgen del Rocío; and §Departamento de Psicología Experimental, Facultad de Psicología, Universidad de Sevilla, Sevilla, Spain.

Conflicts of interest and sources of funding: This work was supported by the Instituto de Salud Carlos III-Fondo Europeo de Desarrollo Regional (ISCIII-FEDER) (PI14/01823, PI16/01575, PI18/01898, PI19/01576), the Consejería de Economía, Innovación, Ciencia y Empleo de la Junta de Andalucía (CVI-02526, CTS-7685), the Consejería de Salud y Bienestar Social de la Junta de Andalucía (PI-0471-2013, PE-0210-2018, PI-0459-2018, PE-0186-2019), and the Fundación Alicia Koplowitz. M.A. L.-E. is supported by VI-PPIT-US from the University of Seville (USE-19094-G). M.J.G. is supported by the “Miguel Servet” program (CP19/00031), J.F.M.-R. is supported by the “Sara Borrell” program (CD13/00229) and VI-PPIT-US from the University of Seville (USE-18817-A), S. J. by the “Juan Rodés” program (B-0007-2019), and D.M.-G. by the “Río Hortega” program (CM18/00142).

Ethical approval was granted by the ethics committee of Hospital Universitario Virgen del Rocío, Universidad de Sevilla, as well as the institutional review boards of the different research centers participating in the Parkinson Progression Marker's Initiative.

Written informed consent was obtained from all study participants and/or authorized representatives.

Correspondence to: Pablo Mir, PhD, or Michel J. Grothe, PhD, Unidad de Trastornos del Movimiento, Instituto de Biomedicina de Sevilla (IBIS), Hospital Universitario Virgen del Rocío, Avda. Manuel Siurot s/n, 41013, Seville, Spain. E-mail: pmir@us.es; mgrothe@us.es.

Copyright © 2021 Wolters Kluwer Health, Inc. All rights reserved.

ISSN: 0363-9762/21/0000-0000

DOI: 10.1097/RLU.0000000000003609

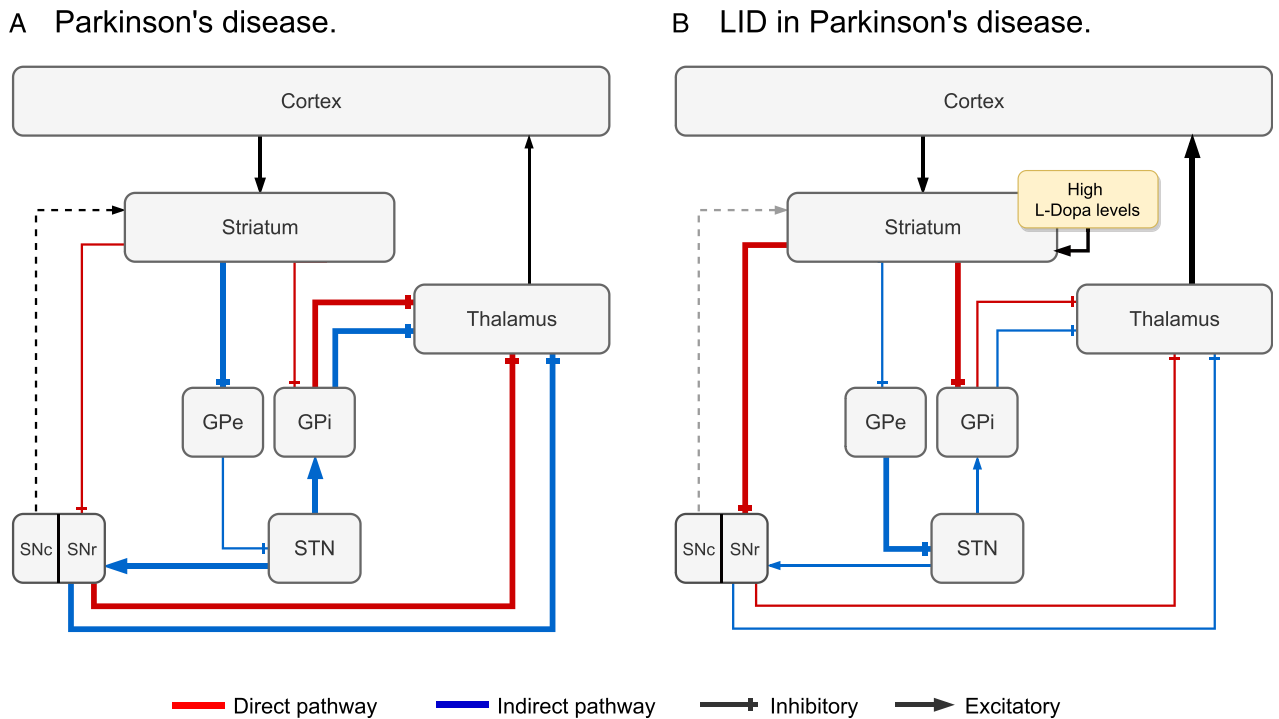


FIGURE 1. Synaptic striatocortical connections assumed to be involved in the pathophysiology of LID. Diagram illustrating the direct (red) and indirect (blue) basal ganglia pathways and their assumed role in the pathophysiology of PD and LID. **A**, In PD, the loss of dopaminergic signaling from the SNc is thought to reduce activity of the direct pathway and to increase activity of the indirect pathway, which together leads to excessive activation of the (inhibitory) output nuclei (GPi/SNr). This in turn results in overinhibition (thick red lines) of thalamic-cortical neurons and consequent suppression of movement. **B**, By contrast, LID is assumed to stem from an excessive dopaminergic stimulation specifically of the direct pathway (thick red lines), which leads to increased inhibition of the output nuclei (GPi/SNr) and thus an abnormal overactivation of thalamocortical neurons.¹³ Arrowheads indicate excitatory connections; perpendicular endings indicate inhibitory connections. SNc, substantia nigra pars compacta; SNr, substantia nigra pars reticulata; GPe, globus pallidus pars externa; GPi, globus pallidus pars interna; STN, subthalamic nucleus.

limited to putaminal regions but also involves caudate areas.¹⁷ Another study found that the caudate asymmetry index, but not the putamen asymmetry index, predicted an increased risk of LID development.¹⁸ Interestingly, a recent study in de novo PD patients could not find significant differences in baseline DAT levels of the anterior putamen, posterior putamen, or caudate, between patients who later developed LID compared with those who did not, indicating that these rather broadly defined anatomical divisions of the striatum may not be sensitive enough to reliably detect subtle LID-associated DAT changes in this early disease stage.¹⁹

Although the neuroanatomy of the striatum is broadly divided into the caudate nucleus, putamen, and nucleus accumbens,^{20,21} axonal tracing experiments in animal models have shown that specific striatal subregions related to different motor, sensory, limbic, and executive functions can be discriminated based on their distinct cortical connectivity profiles within the cortico - basal ganglia - thalamocortical loop.²²⁻²⁴ Accordingly, more recent in vivo MRI-based connectivity studies in humans could demonstrate a similar differential functional architecture of the striatum based on its region-specific cortical connectivity profiles.^{25,26} A study by Tziortzi et al²⁷ used such striatocortical connectivity information derived from diffusion tensor imaging to develop a regionally detailed striatal atlas in standard stereotactic space that subdivides the striatum into functional subregions based on their cortical connectivity profile. Importantly, in a subsequent

pharmacologic PET imaging study, the authors could validate the functional relevance of their connectivity-based striatal atlas by demonstrating that the spatial distribution of D-amphetamine-induced dopamine release more closely corresponded to the connectivity-based functional striatal subregions as compared with the classical structural subdivisions. Based on the distinct cortical connectivity profiles, the atlas distinguishes 3 main functional striatal subdivisions related to limbic, executive, and sensorimotor systems, respectively, and further subdivides the sensorimotor division into 3 distinct subregions specifically related to rostral-motor, caudal-motor, and parietal cortical areas.

In the present study, we used this detailed atlas to assess LID-associated DAT changes within functionally defined striatal subregions. We hypothesized that the development of LID may be specifically related to DAT changes in striatal subregions that are associated with sensorimotor functions, as opposed to cognition-related subregions. In a first analysis, we studied differences in regional DAT levels between PD patients with and without LID using cross-sectional ¹²³I-FP-CIT SPECT data from our local monocentric cohort of PD patients with varying degrees of disease evolution. For validation of the region-specific effects and assessment of the evolution of LID-associated DAT changes from an early disease stage, we also studied longitudinal ¹²³I-FP-CIT SPECT data in relation to LID occurrence in de novo PD patients from the Parkinson Progression Marker's Initiative (PPMI) cohort.

PATIENTS AND METHODS

Participants and Clinical Assessment

Our primary study sample was derived from a local cohort of PD patients recruited at the Movement Disorders Unit of the Hospital Universitario Virgen del Rocío (HUVR) in Seville, which is a regional reference center for movement disorders in southern Spain. The HUVR cohort includes PD patients who were diagnosed with idiopathic PD between 2008 and 2019 following the Movement Disorder Society Clinical Diagnostic Criteria.²⁸ In the present study, we included 185 PD patients from this cohort based on the availability of a ¹²³I-FP-CIT SPECT scan, which was acquired on average 2.67 ± 1.9 years after initial diagnosis and before the occurrence of LID. Over a mean available follow-up of 6.84 ± 1.82 years from initial diagnosis, 73 patients (39.5%) presented LID (PD + LID) at clinical examination, and 112 patients did not (PD-LID). Disease severity was evaluated by the Hoehn and Yahr (H&Y) scale, and dopaminergic therapy was evaluated by L-DOPA equivalent doses (LED), LED of dopaminergic agonists, and total LED.

As an independent validation cohort, we included 343 de novo PD patients from the PPMI. The PPMI is a longitudinal multicenter cohort study designed to investigate the progression of clinical features, as well as neuroimaging and biological markers in de novo PD patients as compared with healthy controls. It is a public-private partnership funded by the Michael J. Fox Foundation for PD research. For up-to-date information on the PPMI study, visit www.ppmi-info.org. In the present study, patients were selected from this cohort based on the availability of a ¹²³I-FP-CIT SPECT scan at baseline and at least 1 follow-up visit. Longitudinal SPECT acquisitions in the PPMI study are scheduled for the first-, second-, and fourth-year study visits, and the included participants in the present study had a median of 3 SPECT scans over a mean follow-up time of 1.83 ± 0.84 years. Patients with PD were categorized as PD + LID if they developed LID over the available clinical follow-up (6.09 ± 1.86 years), as evaluated by the respective item of the Unified Parkinson's Disease Rating Scale (UPDRS) Part IV. This was the case for a total of 161 patients (46.9%), who developed LID on average 4.15 ± 1.83 years after study inclusion. Disease severity was evaluated by the H&Y scale and motor symptom severity by the UPDRS Part III. Analogously to the procedures in the HUVR cohort, dopaminergic therapy was evaluated by doses of L-DOPA, LED by dopaminergic agonists, and total LED.

Neuroimaging Acquisition

Imaging acquisition in both cohorts was performed following similar standardized imaging protocols for the acquisition of ¹²³I-FP-CIT SPECT data.

In the HUVR cohort, SPECT data acquisition was performed on a Siemens Symbia T6 scanner (Siemens Healthcare, Erlangen, Germany) with a dual-head rotating gamma camera and fan-beam collimator. Image acquisition was started between 3 and 4 hours after injection of 185 MBq of ¹²³I-FP-CIT. A total of 120 projections of 30 seconds each over a 360° circular orbit were acquired on a 128 × 128 matrix (zoom 1.23) to build the 3D images. Reconstruction was performed with the Siemens e.soft software (Siemens Healthcare) by filtered back-projection using a Butterworth filter.

SPECT data acquisition in the PPMI cohort was performed across multiple centers following a standardized protocol. Analogous to the HUVR cohort, the image acquisition was acquired 4 ± 0.5 hours following the injection of 111 to 185 MBq of ¹²³I-FP-CIT. Scans were performed with a 128 × 128 matrix stepping

of 3 degrees each for a total of 120 degrees. 3D image reconstruction was then carried out using the PMOD software (PMOD Technologies, Zurich, Switzerland). In order to improve image homogeneity across the multicentric image acquisitions, the Imaging Core Lab of the Institute for Neurodegenerative Disorders (Yale University, New Haven, Conn) applies standardized preprocessing steps to all SPECT acquisitions in PPMI.²⁹ The complete standardized protocol is available at the PPMI website, http://www.ppmi-info.org/wp-content/uploads/2017/06/PPMI-TOM-V8_09-March-2017.pdf. Reconstructed ¹²³I-FP-CIT SPECT scans were downloaded from the PPMI database in March 2018.

Neuroimaging Processing

¹²³I-FP-CIT SPECT processing was carried out in the same way for both cohorts using SPM12 (Wellcome Centre for Human Neuroimaging, Institute of Neurology, UCL, London, United Kingdom) running under MATLAB 2018a (MathWorks, Natick, Mass). SPECT images were first reoriented, setting the anterior commissure as the origin of the coordinate system. Each scan was then spatially normalized into the standard stereotactic MNI (Montreal Neurological Institute) space using a ¹²³I-FP-CIT template developed by our group.³⁰ The resulting images were resliced to a $91 \times 109 \times 91$ matrix of $2 \times 2 \times 2$ -mm³ voxels. The specific ¹²³I-FP-CIT binding ratio (SBR) was calculated for each brain voxel using the following formula: $SBR = [(radioligand\ uptake\ value\ of\ voxel - mean\ radioligand\ uptake\ of\ the\ occipital\ lobe) / radioligand\ uptake\ of\ the\ occipital\ lobe]$.³¹

Functional Striatal Atlas and DAT Quantification

Dopamine transporter levels were quantified by the mean SBR in different functional subregions of the striatum as mapped in the MNI space atlas developed by Tziortzi et al²⁷ (Fig. 2). This atlas subdivides the striatum into subregions based on their differential cortical connectivity patterns with limbic, executive, and sensorimotor areas. Thus, the limbic striatal subregion is connected with the orbital gyrus, gyrus rectus, and subcallosal gyrus/ventral anterior cingulate; the executive subregion with rostral superior and middle frontal gyri and the dorsal prefrontal cortex; and the sensorimotor-related striatum is further subdivided into a rostral-motor subregion with connectivity to rostral area 6, pre-supplementary motor area, and the frontal eye field region; a caudal-motor subregion connected with the precentral gyrus; and a parietal subregion connected with the parietal lobe.

Statistical Analysis

In the primary study, demographic and clinical characteristics of the HUVR cohort were compared between PD-LID and PD + LID groups using 2-sample *t* tests for parametric variables, Mann-Whitney *U* test for nonparametric variables, and the Fisher exact test for categorical variables. Differences in subregional striatal DAT levels between PD-LID and PD + LID groups were assessed with analysis of covariance models controlled for sex, patient age at PD onset, years of disease progression at time of SPECT, H&Y stage, and L-DOPA doses.

In the validation study, baseline demographic and clinical characteristics of the PPMI cohort were compared between PD-LID and PD + LID groups using the same statistical tests as described above for the HUVR cohort. Longitudinal changes in UPDRS-III score and dopaminergic therapy were compared between groups using linear mixed-effects modeling. Analogously, mixed-effect models of longitudinal SPECT measurements were used to investigate the effects of group (PD-LID vs PD + LID) and time and the interaction between group and time on subregional

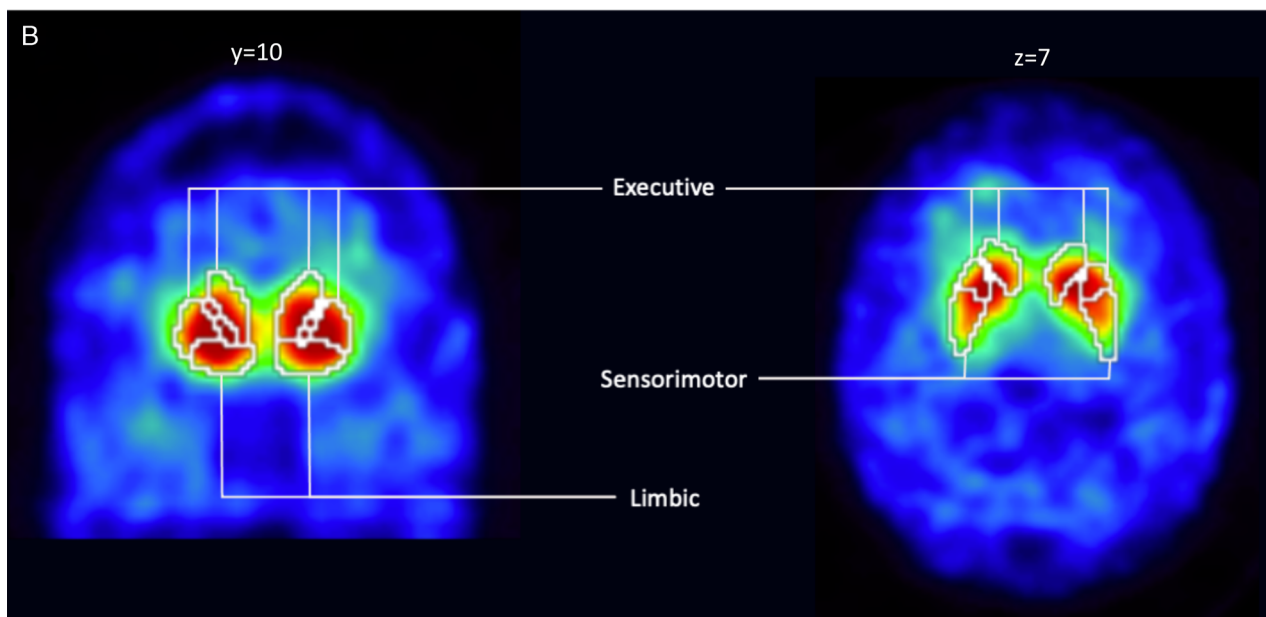
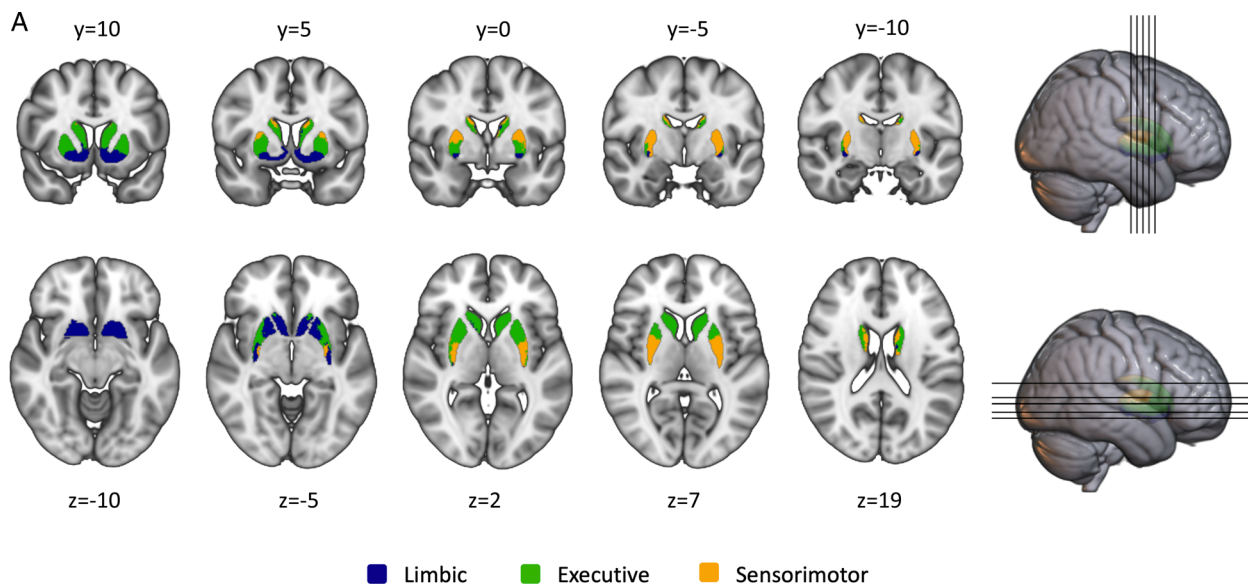


FIGURE 2. Functional striatal subregions and DAT quantification. **A**, Anatomical illustration of the employed atlas of functional striatal subdivisions²⁷ overlaid on representative coronal (top row) and axial (bottom row) sections of a high-resolution MRI template in MNI space. Numbers indicate the respective MNI space coordinates. Colors refer to the different subregions: blue = limbic, green = executive, orange = sensorimotor. **B**, A representation of this atlas in an individual preprocessed ¹²³I-FP-CIT SPECT scan used for automated DAT quantification in the different functional subdivisions.

striatal DAT levels. All mixed-effects models analyzing the subregional striatal DAT levels were controlled for sex, patient age at SPECT, UPDRS-III, and L-DOPA doses. For all models, group, time (in years of SPECT follow-up visit), and the interaction between group and time were included as fixed-effects predictors. Patient ID was included as random effect.

All statistical analyses were conducted in R version 3.5.1 and R Studio 1.2. Linear mixed-effects model analyses were carried out using the lme4 package.

RESULTS

Demographics and Clinical Features of the Local PD Cohort

Demographics and clinical characteristics of the HUVR sample are summarized in Table 1. The mean age at onset of PD was 64.48 ± 11.03 years, and 71 patients (38.4%) were female. There were no significant differences in demographics between PD-LID and PD + LID patients, although the mean age was younger in

TABLE 1. Demographics and Clinical Characteristics of the Local PD Cohort

Variables	PD-LID (n= 112)	PD + LID (n= 73)	Statistics (P)
Gender (female), n (%)	40 (36)	31 (42)	$\chi^2 = 0.59$ (0.443)
Age	65.6 ± 11.35	62.76 ± 10.37	$t = 1.75$ (0.081)
Age at disease onset, y	58.6 ± 11.24	56.16 ± 10.63	$t = 1.48$ (0.139)
Disease duration, y	7.00 ± 1.37	6.59 ± 2.35	$t = 1.33$ (0.186)
Disease duration at SPECT, y	2.75 ± 1.81	2.57 ± 2.03	$t = 0.64$ (0.524)
H&Y stage	2 (2–2.5)	2 (2–2)	$U = 3492$ (0.07)
Levodopa doses	619.48 ± 338.05	946.3 ± 395.19	$t = -5.6$ (<0.001)
LED by agonists	266.89 ± 121.92	306.88 ± 146.72	$t = -1.46$ (0.127)
Total LED	720.68 ± 461.38	1066.81 ± 519.46	$t = -4.62$ (<0.001)

The descriptive values presented are number (%) for female sex, median (IQR) for H&Y stage, and mean ± SD for all other continuous variables. PD-LID, PD patient group who did not develop LID; PD + LID, PD patient group who developed LID; LED, Levodopa equivalent dose.

PD + LID with trend-level statistical significance. PD + LID patients had significantly higher L-DOPA doses ($P < 0.001$) and higher total LED ($P < 0.001$), but did not differ from PD-LID in LED of dopaminergic agonists. There were no significant differences between groups in any other clinical features.

Differences in DAT Levels of Functional Striatal Subregions Between PD-LID and PD + LID Patients in the Local PD Cohort

Mean DAT levels for each group in limbic, executive, and whole sensorimotor, as well as rostral-motor, caudal-motor, and parietal striatal subregions, are summarized in Table 2. As hypothesized, mean DAT levels in sensorimotor-related striatal subregions were significantly lower in the PD + LID group compared with the PD-LID group: whole sensorimotor ($F = 5.99$, $P = 0.016$), rostral-motor ($F = 4.51$, $P = 0.035$), caudal-motor ($F = 5.70$, $P = 0.018$), and parietal ($F = 6.73$, $P = 0.01$). Moreover, mean DAT levels in the executive-related striatal subregion were also significantly lower in PD + LID compared with PD-LID ($F = 5.30$, $P = 0.023$). Group differences in DAT levels in the limbic-related striatal subregion reached only trend-level statistical significance ($F = 3.33$, $P = 0.07$).

Demographics and Clinical Features of PD-LID and PD + LID Patients in the PPMI Cohort

Demographics and clinical characteristics of the validation cohort of de novo PD patients are summarized in Table 3. The mean age at onset of PD was significantly earlier in the PD + LID group compared with the PD-LID group (59.8 ± 9.4 vs 62.3 ± 9.8 , $P = 0.015$). PD + LID patients also had significantly higher baseline UPDRS-III score (22.1 ± 8.3 vs 19.4 ± 9.2 , $P = 0.003$) and H&Y stage (1.5 [interquartile range {IQR}, 1–2] vs 2 with [IQR, 1–2]; $P = 0.033$) than PD-LID patients. There were no significant differences between groups in any other demographic or clinical features at baseline.

Longitudinal changes in motor symptoms and dopaminergic therapy of the PD + LID and PD-LID groups are illustrated in Figure 3. In mixed linear models, the UPDRS-III score was on average significantly higher in PD + LID patients compared with PD-LID patients (effect of group: $\beta = 3.14$, $t = 2.96$, $P = 0.003$). The UPDRS-III scores significantly increased over time in both groups (effect of time: $\beta = 2.64$, $t = 12.85$, $P < 0.001$), but this increase was less pronounced for the PD + LID group (group × time interaction: $\beta = -0.69$, $t = -2.35$, $P = 0.018$).

There was a significant group effect on L-DOPA doses and total LED, being significantly higher in PD + LID patients compared with PD-LID patients since first year of drug initiation (L-DOPA doses: $\beta = 95.19$, $t = 2.27$, $P = 0.023$; total LED: $\beta = 112.80$, $t = 2.65$, $P = 0.008$). Levodopa doses and total LED significantly increased over time in both groups (L-DOPA doses: $\beta = 67.10$, $t = 8.39$, $P < 0.001$; total LED: $\beta = 88.38$, $t = 10.99$, $P < 0.001$), but this increase was significantly higher in the PD + LID group compared with the PD-LID group (group × time interaction: L-DOPA doses: $\beta = 32.7$, $t = 2.89$, $P = 0.004$; total LED: $\beta = 26.96$, $t = 2.37$, $P = 0.018$). L-DOPA equivalent doses of dopaminergic agonists were not significantly different between groups.

Differences in DAT Levels of Functional Striatal Subregions Between PD-LID and PD + LID Patients in the PPMI Cohort

Baseline and longitudinal measurements of subregional striatal DAT measurements in the PD + LID and PD-LID groups from the PPMI cohort are summarized in Table 4 and illustrated in Figure 4. After correcting for sex, age at SPECT, UPDRS-III, and L-DOPA doses, DAT levels in the sensorimotor-related striatal subregion were significantly lower in PD + LID patients compared with PD-LID patients (group effect: $\beta = -0.06$, $t = -2.05$, $P = 0.041$), but no significant group effects were observed for the limbic- and executive-related striatal subregions. Among the

TABLE 2. Mean Regional Striatal DAT Binding in the Local PD Cohort

Striatal Subregions	PD-LID (n= 112)	PD + LID (n= 73)	Cohen <i>d</i>	F (P)
Limbic	2.19 ± 0.34	2.1 ± 0.3	0.27	3.33 (0.07)
Executive	2.22 ± 0.42	2.1 ± 0.36	0.31	5.30 (0.023)
Sensorimotor	1.86 ± 0.33	1.74 ± 0.26	0.38	5.99 (0.016)
Rostral motor	2.12 ± 0.42	1.99 ± 0.35	0.33	4.51 (0.035)
Caudal motor	1.85 ± 0.33	1.73 ± 0.26	0.38	5.70 (0.018)
Parietal	1.66 ± 0.28	1.55 ± 0.22	0.41	6.73 (0.01)

The descriptive values presented are mean SBR ± SD, the Cohen *d* effect size for (unadjusted) group differences between PD-LID and PD + LID, and analysis of covariance statistics.

PD-LID, PD patient group who did not develop LID; PD + LID, PD patient group who developed LID.

TABLE 3. Demographics and Clinical Characteristics of the PPMI Cohort

Variables	PD-LID (n= 182)				PD + LID (n = 161)			
	BL	1st Visit	2nd Visit	4th Visit	BL	1st Visit	2nd Visit	4th Visit
Gender	64 (35%)	—	—	—	53 (33%)	—	—	—
Age	62.87 (9.93)	63.57 (10.05)	64.78 (10.2)	67.20 (10.23)	60.25 (9.45)	61.26 (9.34)	62.84 (9.49)	65.09 (8.90)
Disease duration years	0.57 (0.55)	1.73 (0.61)	2.65 (0.53)	4.6 (0.55)	0.49 (0.5)	1.57 (0.52)	2.58 (0.55)	4.61 (0.53)
UPDRS III	19.37 (9.15)	23.15 (10.04)	27.35 (11.81)	28.11 (10.6)	22.11 (8.25)	25.73 (10.51)	26.32 (9.87)	30.59 (10.84)
Levodopa doses	—	63.49 (165.27)	136.52 (224.29)	269.18 (269.58)	—	177.86 (306.56)	318.04 (391.34)	484.31 (450.16)
Dopamine agonist LED	—	46.46 (85.2)	74.44 (117.1)	89.46 (116.88)	—	44.95 (85.12)	66.17 (116.71)	84.14 (136.52)
Total LED	—	153.36 (189.18)	273.88 (231.13)	430.57 (265.7)	—	268.68 (303.04)	461.01 (392.23)	634.49 (454.18)

The descriptive values presented are number (%) for female sex and mean (SD) for all other continuous variables.
 PD-LID, PD patient group who did not develop LID; PD + LID, PD patient group who developed LID; BL, baseline visit; LED, Levodopa equivalent dose.

different sensorimotor-related striatal subregions, DAT levels in rostral-motor ($\beta = -0.08, t = -2.14, P = 0.033$) and caudal-motor ($\beta = -0.06, t = -1.975, P = 0.049$) subregions were significantly lower in PD + LID than PD-LID patients, but group differences in the parietal subregion were only trend-level significant ($\beta = -0.04, t = -1.86, P = 0.064$).

Dopamine transporter levels in all striatal subregions significantly decreased over time (all time effects, $P < 0.001$), but longitudinal change did not differ between the PD + LID and PD-LID groups in any of the striatal subregions (all group \times time interactions, $P > 0.32$).

DISCUSSION

We investigated DAT changes measured with ¹²³I-FP-CIT SPECT within functionally defined striatal subregions between PD patients who developed LID and those who did not. In a primary study on our local monocentric PD cohort with varying degrees of

disease progression, we found that PD patients who developed LID showed significantly lower DAT levels across large parts of the striatum and specifically in subregions associated with sensorimotor functions. The regional specificity of LID-associated DAT depletion in sensorimotor-related subregions of the striatum could be corroborated in an independent study cohort of longitudinally followed de novo PD patients. Interestingly, analysis of longitudinal ¹²³I-FP-CIT SPECT data in this cohort indicated that the LID-associated differences in sensorimotor striatal DAT levels were already present at the time of initial PD diagnosis, on average 4 years before the development of LID, and group differences were largely constant over time. Together, these results indicate that the development of LID in PD is specifically related to dopaminergic denervation in striatal subregions that are associated with sensorimotor functions and that these changes can be detected at a very early disease stage.

Dopamine transporter depletion in broad anatomically defined caudate and putaminal regions^{32,33} has been related to the development of LID in PD patients in several previous studies.^{12,14,15,34}

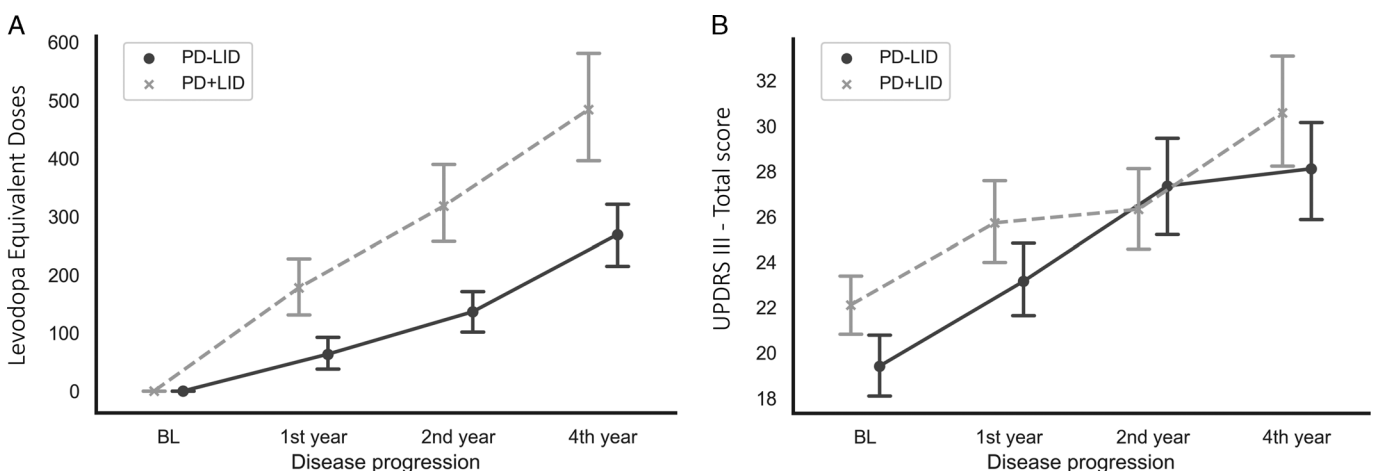


FIGURE 3. Longitudinal changes in UPDRS-III scores and LEDs for PD + LID and PD-LID groups in the PPMI cohort. **A**, Longitudinal LEDs and **(B)** total UPDRS-III score over follow-up time illustrated by the mean value and standard error for each visit. Levodopa doses were significantly higher in PD + LID patients compared with PD-LID patients since first year of drug initiation, and the dosage increase over time was significantly higher in PD + LID patients. The UPDRS-III score was on average significantly higher in PD + LID patients compared with PD-LID patients, although the UPDRS-III score increase over time was less pronounced for the PD + LID group. PD-LID, PD patient group who did not develop LID; PD + LID, PD patient group who developed LID; BL, baseline visit.

TABLE 4. Mean Regional Striatal DAT Binding in Serial SPECT Data From the PPMI Cohort

Striatal Subregions	Group	Descriptive Values				Mixed Linear Model Statistics
		BL	1st Visit	2nd Visit	4th Visit	(β , t , P)
Limbic	PD-LID	2.19 (0.37)	2.12 (0.34)	2.05 (0.36)	1.93 (0.33)	a. $\beta = -0.03$, $t = -0.84$, $P = 0.40$
	PD + LID	2.18 (0.33)	2.08 (0.36)	1.99 (0.34)	1.86 (0.32)	b. $\beta = -0.05$, $t = -7.38$, $P < 0.001$ c. $\beta = -0.004$, $t = -0.53$, $P = 0.60$
Executive	PD-LID	2.23 (0.39)	2.15 (0.36)	2.04 (0.39)	1.89 (0.35)	a. $\beta = -0.05$, $t = -1.23$, $P = 0.22$
	PD + LID	2.21 (0.36)	2.09 (0.39)	1.97 (0.37)	1.83 (0.36)	b. $\beta = -0.07$, $t = -9.38$, $P < 0.001$ c. $\beta = -0.0004$, $t = -0.05$, $P = 0.96$
Sensorimotor	PD-LID	1.84 (0.29)	1.78 (0.27)	1.70 (0.29)	1.60 (0.25)	a. $\beta = -0.06$, $t = -2.05$, $P = 0.041$
	PD + LID	1.80 (0.25)	1.71 (0.25)	1.63 (0.24)	1.53 (0.23)	b. $\beta = -0.05$, $t = -10.27$, $P < 0.001$ c. $\beta = 0.005$, $t = 0.77$, $P = 0.44$
Rostral motor	PD-LID	2.13 (0.37)	2.03 (0.35)	1.93 (0.37)	1.81 (0.33)	a. $\beta = -0.08$, $t = -2.14$, $P = 0.033$
	PD + LID	2.05 (0.33)	1.95 (0.33)	1.83 (0.32)	1.70 (0.32)	b. $\beta = -0.07$, $t = -10.96$, $P < 0.001$ c. $\beta = 0.005$, $t = 0.57$, $P = 0.57$
Caudal motor	PD-LID	1.82 (0.29)	1.77 (0.27)	1.69 (0.30)	1.58 (0.26)	a. $\beta = -0.06$, $t = -1.975$, $P = 0.049$
	PD + LID	1.78 (0.25)	1.69 (0.25)	1.61 (0.25)	1.51 (0.23)	b. $\beta = -0.05$, $t = -9.53$, $P < 0.001$ c. $\beta = 0.01$, $t = 0.74$, $P = 0.46$
Parietal	PD-LID	1.64 (0.23)	1.59 (0.21)	1.54 (0.24)	1.45 (0.20)	a. $\beta = -0.04$, $t = -1.86$, $P = 0.064$
	PD + LID	1.61 (0.20)	1.55 (0.21)	1.48 (0.20)	1.41 (0.17)	b. $\beta = -0.04$, $t = -8.70$, $P < 0.001$ c. $\beta = 0.0$, $t = 0.99$, $P = 0.32$

The descriptive values presented are mean SBR (SD). Mixed-linear model statistics are (a) group effect, (b) time effect, and the (c) group \times time interaction.

PD-LID, PD patient group who did not develop LID; PD + LID, PD patient group who developed LID; BL, baseline visit.

However, these studies had not differentiated between distinct functionally defined striatal subregions, which may be differentially implicated in different aspects of the clinical symptoms in PD.³⁵⁻³⁷ In agreement with previous experimental studies in animal models,^{38,39} our in vivo imaging findings confirm that dopaminergic degeneration associated with the occurrence of LID specifically implicates striatal areas connected to the cortical sensorimotor system.

Furthermore, in an independent validation study using data from the PPMI cohort, we found that excess DAT reductions in de novo PD patients who later developed LID were limited to the sensorimotor striatal region and that this difference was already present at study baseline (coinciding with initial PD diagnosis) and remained largely constant over an average of 1.8 years of follow-up with SPECT imaging. Our results agree with previous studies that have shown the predictive role of decreased putaminal DAT levels for the development of LID in de novo PD patients using both the PPMI¹⁷ and other cohorts.^{14,15} However, these findings contrast with other studies that could not fully reproduce this predictive effect in de novo PD patients,¹⁹ including a recent study using data from the PPMI cohort.¹⁸ This latter study investigated a wide range of possible risk factors for the development of LID, and although they could confirm several previously reported risk factors for LID, they did not find significant differences in baseline DAT uptake levels of the caudate or putamen between patients who did or did not develop LID. However, somewhat surprisingly, and in contrast to other studies on LID-associated DAT changes,¹⁶ the caudate asymmetry index, but not the putamen asymmetry index, was found to predict an increased risk of LID development in this study. Possible explanations for the discrepancy with our current findings on LID development in the PPMI cohort include the use of longitudinal SPECT data and its statistical modeling using mixed linear models, whereas only baseline SPECT-derived DAT values were used in this previous study. However, another explanation may be that the rather broad anatomical divisions of the striatum (caudate and putamen) used in this previous study may not be sensitive enough to reliably detect subtle LID-associated DAT changes in this early disease stage (see Supplemental Data for a complementary

analysis of standard caudate and putamen regions of interest in our data sets that corroborate this notion (Supplemental Digital Content 1, <http://links.lww.com/CNM/A315>).

Taken together, our findings across 2 independent cohorts of PD patients at varying stages of disease evolution suggest that the development of LID may be specifically associated with reduced DAT levels in functionally defined sensorimotor-related striatal subregions. These subregions are defined by their specific cortical connectivity pattern with cortical motor areas including rostral Brodmann area 6, pre-supplementary motor area, precentral gyrus, and the frontal eye field region.²⁷ Interestingly, recent diffusion tensor imaging and resting-state functional MRI studies have shown abnormal striatocortical connectivity patterns in PD patients who suffer from LID, especially affecting connections between the putamen and cortical sensorimotor areas.⁴⁰⁻⁴² Moreover, in a pharmacodynamic functional neuroimaging approach that mapped the effect of a single dose of L-DOPA on connectivity in cortico-basal ganglia motor loops, it could be shown that the dopaminergic modulation of feedback connections from the putamen to cortical motor areas was strongly involved in the development and severity of LID, but not the forward connections from cortical motor areas to the putamen.⁴³ Our findings on specific LID-associated DAT level depletion in functional subregions of the striatum that are connected to sensorimotor cortical areas may represent a neurodegenerative correlate of this abnormal dopaminergic modulation of cortical motor areas through striatal projections. However, additional multimodal imaging studies are necessary to investigate the relation between regionally specific DAT depletion and striatocortical connectivity changes in the development of LID.

Although the LID-associated differences in striatal DAT levels showed highest effect size in the sensorimotor striatal subregions, it should be noted that in our primary study cohort these differences also extended into the executive striatal subregion. These results could be related to recent findings reported by Yoo et al,⁴⁴ who demonstrated that LID development was closely associated with the progression of cognitive decline, especially with frontal executive dysfunction. Interestingly, a recent multimodal ¹²³I-FP-CIT SPECT and [¹⁸F]FDG-PET imaging study found that reduced DAT levels

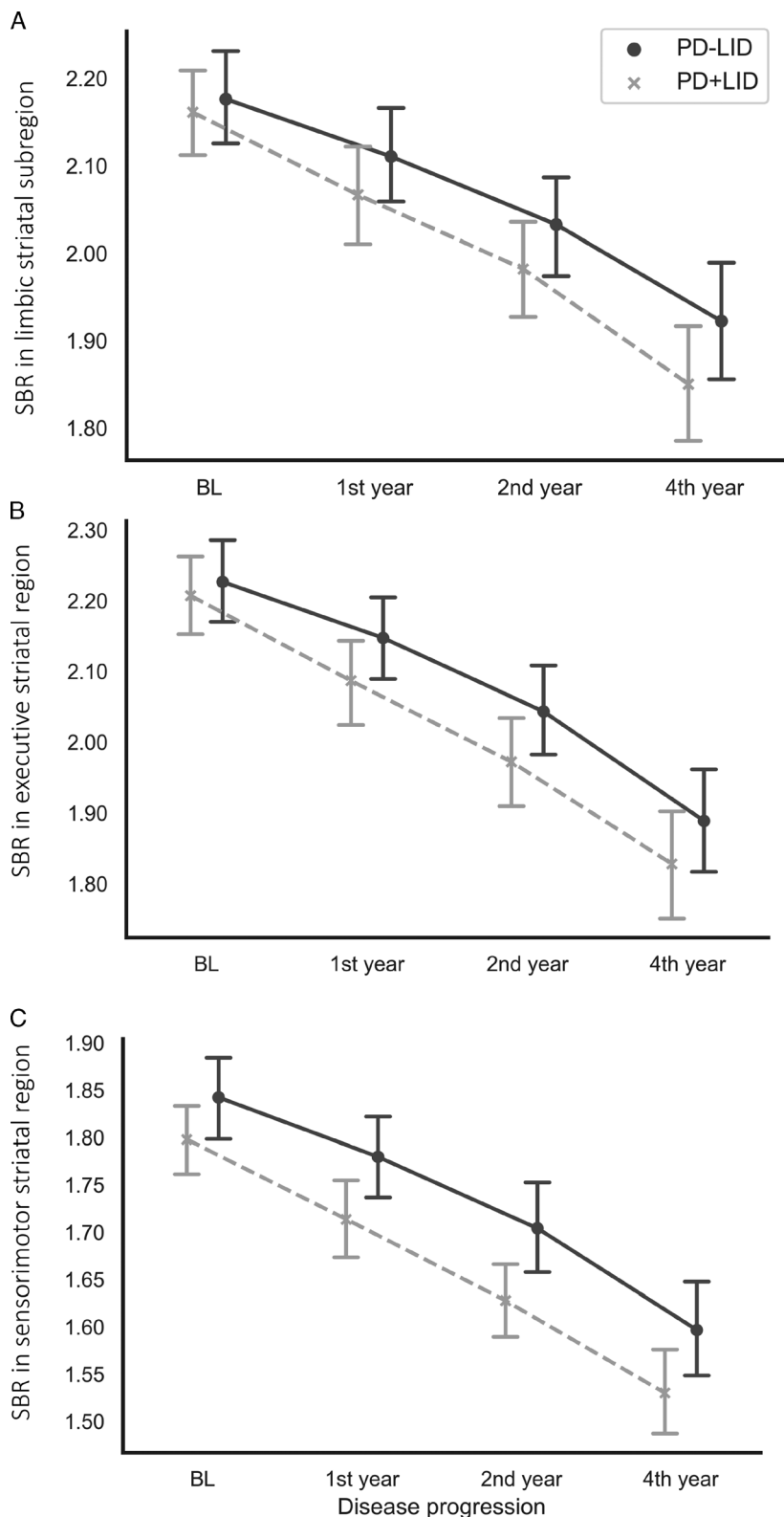


FIGURE 4. Longitudinal DAT binding changes in striatal subregions for PD + LID and PD-LID groups in the PPMI cohort. DAT changes in the (A) limbic, (B) executive, and (C) sensorimotor striatal region over follow-up time illustrated by the mean value and standard error for each visit. DAT levels in the sensorimotor-related striatal subregion were significantly lower in PD + LID patients compared with PD-LID patients, but no significant differences were observed for the limbic- and executive-related striatal subregions. PD-LID, PD patient group who did not develop LID; PD + LID, PD patient group who developed LID; BL, baseline visit.

in the cognitive part of the striatum (combined executive + limbic subregions), but not in the sensorimotor part, are associated with frontomedial hypometabolism in PD patients, which likely represents a neurofunctional correlate of impaired executive functions.⁵⁵ Together with our findings of a selective association of LID with DAT depletion in sensorimotor regions in drug-naïve de novo PD patients, these data could indicate a sequence of LID-associated DAT changes progressing from sensorimotor to executive striatal subregions with corresponding clinical-cognitive changes. Molecular neuroimaging studies over longer follow-up intervals will be necessary to study the regionally progressive neurodegenerative changes underlying LID-associated cognitive changes in more detail.

As expected, in both study cohorts, we found higher doses of L-DOPA and total LED in PD patients who suffered LID compared with PD patients who did not develop this complication. Moreover, PD patients with LID also had more severe motor symptoms than PD patients without LID. These results are fully consistent with previous findings on common risk factors of LID, indicating a narrowing of the therapeutic window of L-DOPA treatment with progression of motor symptoms in PD.^{45,46} Interestingly, in the PPMI cohort, we also observed a higher longitudinal increase of L-DOPA doses in PD patients who develop LID, whereas DAT levels in the sensorimotor-related striatal subregion were already significantly reduced at baseline compared with the PD-LID group and remained relatively constant over time. This corroborates previously reported interactive effects of L-DOPA treatment and dopaminergic depletion on LID, where high doses of L-DOPA specifically associate with dyskinesia in patients with higher levels of dopaminergic depletion.^{47,48}

Our data suggest that the proposed method of measuring DAT depletion in a functionally defined sensorimotor-related striatal region may provide a more sensitive imaging biomarker for detecting LID-associated dopaminergic degeneration in an early disease stage and may thus improve the individual prognosis of, and clinical decision making for, this common medication-related complication in PD.^{14,15,18,49} Taking into account other known clinical risk factors, the assessment of an individual patient's LID risk through the specific measurement of sensorimotor-related striatal dopaminergic depletion at an early disease stage could help the clinician in therapeutic decision making and potentially improve prevention and management of this complication through individually adjusted therapeutic strategies.^{50–52} A next step toward successful clinical translation of our current research findings to such a precision medicine approach will involve the development of accurate clinical decision support systems that integrate the information from the proposed molecular imaging biomarker with other clinical and biological sources of information within multivariate predictive models.^{53,54} However, it also has to be noted that our current findings were obtained in a controlled research environment and in patients from highly specialized tertiary care centers, so a further validation in less selected patient cohorts is required. Moreover, the automated analysis methods we use for measuring DAT levels in specific functionally defined striatal subregions require expertise in computational image processing and analysis, which could pose a limitation for the implementation of this measurement in the wider health care system. Nevertheless, we believe that translation of this method outside of dedicated research centers will be feasible through increasingly specialized software solutions that are becoming available for medical image analysis in clinical settings.^{55,56} A wider clinical accessibility of our proposed regional DAT quantification method through such user-friendly software solutions will allow testing the prognostic potential of this method as a molecular imaging biomarker for increased LID risk through a diagnostic trial in a real-world clinical setting.

A principal limitation of our study is that the data from our local cohort were collected in a retrospective manner. The occurrence

of LID was evaluated by clinical examination through neurologists specialized in movement disorders, but no additional standardized scales for the assessment of motor complications in PD (such as the UPDRS-IV or Abnormal Involuntary Movement Scale) were available, so that more detailed analyses of dyskinesia severity or type of dyskinetic complication could not be performed.^{48,57,58} Moreover, quantification of specific DAT binding reductions in spatially detailed striatal subregions may benefit from partial volume correction of ¹²³I-FP-CIT SPECT signal using anatomic information from high-resolution structural MRI,⁵⁹ but these data were not available for our retrospective cohort. In general, the spatial resolution of ¹²³I-FP-CIT SPECT scans may cast doubt on the ability of this imaging modality to discern signal from relatively small striatal subregions, particularly with respect to the distinct sensorimotor-related subdivisions defined in the employed striatal connectivity atlas.²⁷ However, we observed reproducible differences in relation to LID-associated DAT depletion in the larger sensorimotor-related region compared with the cognition-related regions across 2 independent cohorts. Finally, other neuronal systems⁶⁰ and the influence of other neurotransmitters,⁶¹ such as alterations in serotonin levels,^{62,63} could be involved in the pathophysiology of LID, but could not be taken into account in our current study.

In summary, we provide evidence that the development of LID in PD specifically associates with dopaminergic depletion in distinct sensorimotor-related subregions of the striatum. Measuring DAT depletion in these functionally defined regions of interest may provide a more sensitive tool to detect LID-associated dopaminergic changes in an early disease stage, and could thus improve individual prognosis of, and clinical decision making for, this common complication in PD symptoms. Studying the relation of region-specific striatal dopaminergic denervation with functional changes in striatocortical signaling loops and their interaction with others pathophysiologic factors measurable by neuroimaging, such as nondopaminergic neurotransmitter deficits or region-specific atrophic brain changes, provides an exciting venue for future research into the complex pathophysiologic mechanisms underlying LID in PD.

ACKNOWLEDGMENTS

The authors thank all the patients and their caregivers for their efforts to participate in this study. In addition to our local university hospital cohort, data used in the preparation of this article were obtained from the Parkinson Progression Marker's Initiative database (www.ppmi-info.org/data). Parkinson Progression Marker's Initiative—a public-private partnership—is funded by the Michael J. Fox Foundation for Parkinson's Research. Corporate funding partners include AbbVie, Allergan, Amathus, Avid, Biogen, BioLegend, Bristol-Myers Squibb, Celgene, Denali, GE Healthcare, Genentech, GlaxoSmithKline, Janssen Neurosciences, Lilly, Lundbeck, Merck, Meso Scale Discovery, Pfizer, Piramal, Prevail, Roche, Sanofi Genzyme, Servier, Takeda, Teva, UCB, Verily, and Voyager, and philanthropic funding partners include GOLUB CAPITAL.

REFERENCES

- Poewe W, Seppi K, Tanner CM, et al. Parkinson disease. *Nat Rev Dis Prim.* 2017;3:1–21.
- Marsden CD, Parkes JD. "On-off" effects in patients with Parkinson's disease on chronic levodopa therapy. *Lancet.* 1976;307:292–296.
- Péchevis M, Clarke CE, Vieregge P, et al. Effects of dyskinesias in Parkinson's disease on quality of life and health-related costs: a prospective European study. *Eur J Neurol.* 2005;12:956–963.
- Ahlskog JE, Muenter MD. Frequency of levodopa-related dyskinesias and motor fluctuations as estimated from the cumulative literature. *Mov Disord.* 2001;16:448–458.

5. Rascol O, Brooks DJ, Korczyn AD, et al. A five-year study of the incidence of dyskinesia in patients with early Parkinson's disease who were treated with ropinirole or levodopa. *N Engl J Med*. 2000;342:1484–1491.
6. Espay AJ, Morgante F, Merola A, et al. Levodopa-induced dyskinesia in Parkinson disease: current and evolving concepts. *Ann Neurol*. 2018;797–811.
7. Warren Olanow C, Kieburtz K, Rascol O, et al. Factors predictive of the development of levodopa-induced dyskinesia and wearing-off in Parkinson's disease. *Mov Disord*. 2013;28:1064–1071.
8. Grandas F, Galiano ML, Taberner C. Risk factors for levodopa-induced dyskinesias in Parkinson's disease. *J Neurol*. 1999;246:1127–1133.
9. Fahn S, Oakes D, Shoulson I, et al. Levodopa and the progression of Parkinson's disease. *N Engl J Med*. 2004;351:2498–2508.
10. Porras G, de Deurwaerdere P, Li Q, et al. L-DOPA-induced dyskinesia: beyond an excessive dopamine tone in the striatum. *Sci Rep*. 2014;4.
11. De la Fuente-Fernández R, Sossi V, Huang Z, et al. Levodopa-induced changes in synaptic dopamine levels increase with progression of Parkinson's disease: implications for dyskinesias. *Brain*. 2004;127:2747–2754.
12. De la Fuente-Fernández R, Lu JQ, Sossi V, et al. Biochemical variations in the synaptic level of dopamine precede motor fluctuations in Parkinson's disease: PET evidence of increased dopamine turnover. *Ann Neurol*. 2001;49:298–303.
13. Picconi B, Hernández LF, Obeso JA, et al. Motor complications in Parkinson's disease: striatal molecular and electrophysiological mechanisms of dyskinesias. *Mov Disord*. 2018;33:867–876.
14. Hong JY, Oh JS, Lee I, et al. Presynaptic dopamine depletion predicts levodopa-induced dyskinesia in de novo Parkinson disease. *Neurology*. 2014;82:1597–1604.
15. Yoo HS, Chung SJ, Chung SJ, et al. Presynaptic dopamine depletion determines the timing of levodopa-induced dyskinesia onset in Parkinson's disease. *Eur J Nucl Med Mol Imaging*. 2018;45:423–431.
16. Chung SJ, Yoo HS, Lee HS, et al. The pattern of striatal dopamine depletion as a prognostic marker in de novo Parkinson disease. *Clin Nucl Med*. 2018;43:787–792.
17. Jeong EH, Sunwoo MK, Song YS. Serial I-123-FP-CIT SPECT image findings of Parkinson's disease patients with levodopa-induced dyskinesia. *Front Neurol*. 2018;9:1–7.
18. Eusebi P, Romoli M, Paoletti FP, et al. Risk factors of levodopa-induced dyskinesia in Parkinson's disease: results from the PPMI cohort. *npj Park Dis [Internet]*. 2018;4:4. <http://dx.doi.org/10.1038/s41531-018-0069-x>.
19. Roussakis A-A, Gennaro M, Lao-Kaim NP, et al. Dopamine transporter density in de novo Parkinson's disease does not relate to the development of levodopa-induced dyskinesias. *J Neuroinflamm Neurodegener Dis [Internet]*. 2019;3:10000. <http://www.pubmedcentral.nih.gov/articlerender.fcgi?artid=PMC6901354>.
20. Alexander G. Parallel organization of functionally segregated circuits linking basal ganglia and cortex. *Annu Rev Neurosci*. 1986;9:357–381.
21. Haber SN. The primate basal ganglia: parallel and integrative networks. *J Chem Neuroanat*. 2003;26:317–330.
22. Alexander GE, Crutcher MD, DeLong MR. Chapter 6 basal ganglia-thalamocortical circuits: parallel substrates for motor, oculomotor, "prefrontal" and "limbic" functions. *Prog Brain Res*. 1991;85:119–146.
23. Parent A, Hazrati LN. Functional anatomy of the basal ganglia. I. The cortico-basal ganglia-thalamo-cortical loop. *Brain Res Rev*. 1995;91–127.
24. DeLong MR, Wichmann T. Circuits and circuit disorders of the basal ganglia. *Arch Neurol*. 2007;64:20–24.
25. Choi EY, Thomas Yeo BT, Buckner RL. The organization of the human striatum estimated by intrinsic functional connectivity. *J Neurophysiol*. 2012;108:2242–2263.
26. Draganski B, Kherif F, Klöppel S, et al. Evidence for segregated and integrative connectivity patterns in the human basal ganglia. *J Neurosci*. 2008;28:7143–7152.
27. Tziortzi AC, Haber SN, Searle GE, et al. Connectivity-based functional analysis of dopamine release in the striatum using diffusion-weighted MRI and positron emission tomography. *Cereb Cortex*. 2014;24:1165–1177.
28. Postuma RB, Berg D, Stern M, et al. MDS clinical diagnostic criteria for Parkinson's disease. *Mov Disord*. 2015;30:1591–1601.
29. Seibyl J, Marek K, Zupal IG. The role of the core imaging laboratory in multicenter trials. *Semin Nucl Med*. 2010;38:338–346.
30. García-Gómez FJ, García-Solís D, Luis-Simón FJ, et al. Elaboration of the SPM template for the standardization of SPECT images with ¹²³I-Ioflupane. *Rev Esp Med Nucl Imagen Mol English Ed*. 2013;32:350–356.
31. Innis RB, Cunningham VJ, Delforge J, et al. Consensus nomenclature for in vivo imaging of reversibly binding radioligands. *J Cereb Blood Flow Metab*. 2007;27:1533–1539.
32. Morrish PK, Sawle GV, Brooks DJ. Regional changes in [¹⁸F]dopa metabolism in the striatum in Parkinson's disease. *Brain*. 1996;119:2097–2103.
33. Nandhagopal R, Kuramoto L, Schulzer M, et al. Longitudinal progression of sporadic Parkinson's disease: a multi-tracer positron emission tomography study. *Brain*. 2009;132:2970–2979.
34. De la Fuente-Fernández R, Pal PK, Vingerhoets FJG, et al. Evidence for impaired presynaptic dopamine function in parkinsonian patients with motor fluctuations. *J Neural Transm*. 2000;107:49–57.
35. Apostolova I, Lange C, Frings L, et al. Nigrostriatal degeneration in the cognitive part of the striatum in Parkinson disease is associated with frontomedial hypometabolism. *Clin Nucl Med*. 2020;45:95–99.
36. Khan AR, Hiebert NM, Vo A, et al. Biomarkers of Parkinson's disease: striatal sub-regional structural morphometry and diffusion MRI. *Neuroimage Clin*. 2019;21:101597.
37. Kübler D, Schroll H, Buchert R, et al. Cognitive performance correlates with the degree of dopaminergic degeneration in the associative part of the striatum in non-demented Parkinson's patients. *J Neural Transm*. 2017;124:1073–1081.
38. Wong MY, Borgkvist A, Choi SJ, et al. Dopamine-dependent corticostriatal synaptic filtering regulates sensorimotor behavior. *Neuroscience*. 2015;290:594–607.
39. Bamford NS, Robinson S, Palmiter RD, et al. Dopamine modulates release from corticostriatal terminals. *J Neurosci*. 2004;24:9541–9552.
40. Herz DM, Haagensen BN, Christensen MS, et al. The acute brain response to levodopa heralds dyskinesias in Parkinson disease. *Ann Neurol*. 2014;75:829–836.
41. Herz DM, Haagensen BN, Nielsen SH, et al. Resting-state connectivity predicts levodopa-induced dyskinesias in Parkinson's disease. *Mov Disord*. 2016;31:521–529.
42. Wang L, Wang M, Si Q, et al. Altered brain structural topological properties in Parkinson's disease with levodopa-induced dyskinesias. *Park Relat Disord*. 2019;67:36–41.
43. Herz DM, Haagensen BN, Christensen MS, et al. Abnormal dopaminergic modulation of striato-cortical networks underlies levodopa-induced dyskinesias in humans. *Brain*. 2015;138:1658–1666.
44. Yoo HS, Chung SJ, Lee YH, et al. Levodopa-induced dyskinesia is closely linked to progression of frontal dysfunction in PD. *Neurology*. 2019;92:E1468–E1478.
45. Angela Cenci M. Presynaptic mechanisms of L-DOPA-induced dyskinesia: the findings, the debate, the therapeutic implications. *Front Neurol*. 2014;5:1–15.
46. Hauser RA, McDermott MP, Messing S. Factors associated with the development of motor fluctuations and dyskinesias in Parkinson disease. *Arch Neurol*. 2006;63:1756–1760.
47. Francardo V, Recchia A, Popovic N, et al. Impact of the lesion procedure on the profiles of motor impairment and molecular responsiveness to L-DOPA in the 6-hydroxydopamine mouse model of Parkinson's disease. *Neurobiol Dis*. 2011;42:327–340.
48. Putterman DB, Munhall AC, Kozell LB, et al. Evaluation of levodopa dose and magnitude of dopamine depletion as risk factors for levodopa-induced dyskinesia in a rat model of Parkinson's disease. *J Pharmacol Exp Ther*. 2007;323:277–284.
49. Schapira AHV. A pragmatic, personalised approach to treatment initiation in Parkinson's disease. *Lancet Neurol*. Elsevier Ltd; 2020;19:376–378.
50. De Bie RMA, Clarke CE, Espay AJ, et al. Initiation of pharmacological therapy in Parkinson's disease: when, why, and how. *Lancet Neurol*. 2020;19:452–461.
51. Fox SH, Katzenschlager R, Lim SY, et al. International Parkinson and movement disorder society evidence-based medicine review: update on treatments for the motor symptoms of Parkinson's disease. *Mov Disord*. 2018;33:1248–1266.
52. Worth PF. When the going gets tough: how to select patients with Parkinson's disease for advanced therapies. *Pract Neurol*. 2013;13:140–152.
53. Klucken J, Kruger R, Schmidt P, et al. Management of Parkinson's disease 20 years from now: towards digital health pathways. *J Parkinsons Dis*. 2018;8:S85–S94.
54. Zubair R, Francisco G, Rao B. Artificial intelligence for clinical decision support. *Brain*. 2018;102:210–211.
55. López-González FJ, Silva-Rodríguez J, Paredes-Pacheco J, et al. Intensity normalization methods in brain FDG-PET quantification. *Neuroimage*. 2020;222:117229.

56. Brogley JE. DatQuant: the future of diagnosing Parkinson disease. *J Nucl Med Technol.* 2019;47:21–26.
57. Colosimo C, Martínez-Martín P, Fabbrini G, et al. Task force report on scales to assess dyskinesia in Parkinson's disease: critique and recommendations. *Mov Disord.* 2010;25:1131–1142.
58. Pavese N, Evans AH, Tai YF, et al. Clinical correlates of levodopa-induced dopamine release in Parkinson disease: a PET study. *Neurology.* 2006;67:1612–1617.
59. Trnka J, Dusek P, Samal M, et al. MRI-guided voxel-based automatic semi-quantification of dopamine transporter imaging. *Phys Med.* 2020;75:2–10.
60. Calabresi P, Picconi B, Tozzi A, et al. Direct and indirect pathways of basal ganglia: a critical reappraisal. *Nat Neurosci.* 2014;17:1022–1030.
61. Beaudoin-Gobert M, Météreau E, Duperrier S, et al. Pathophysiology of levodopa-induced dyskinesia: insights from multimodal imaging and immunohistochemistry in non-human primates. *Neuroimage.* 2018;183:132–141.
62. Carta M, Carlsson T, Kirik D, et al. Dopamine released from 5-HT terminals is the cause of L-DOPA-induced dyskinesia in parkinsonian rats. *Brain.* 2007;130:1819–1833.
63. Roussakis AA, Politis M, Towey D, et al. Serotonin-to-dopamine transporter ratios in Parkinson disease. *Neurology.* 2016;86:1152–1158.